27 May 2010, 4:30 pm - 6:20 pm

CPT-Based Comparative Mapping of Liquefaction Hazard for Large Areas

Johann Facciorusso
University of Florence, Italy

Marco Uzielli
Georisk Engineering S.r.l., Italy

Giovanni Vannucchi
University of Florence, Italy


Fifth International Conference on
Recent Advances in Geotechnical Earthquake Engineering and Soil Dynamics
and Symposium in Honor of Professor I.M. Idriss
May 24-29, 2010 • San Diego, California

CPT-BASED COMPARATIVE MAPPING OF LIQUEFACTION HAZARD FOR LARGE AREAS

Johann Facciorusso
Department of Civil and Environmental Engineering, University of Florence,
Via S. Marta,3 - 50139 Florence, Italy.

Marco Uzielli
Georisk Engineering S.r.l.,
Via Giuseppe Giusti 16/5
50121 Florence, Italy.

Giovanni Vannucchi
Department of Civil and Environmental Engineering, University of Florence,
Via S. Marta,3 - 50139 Florence, Italy.

ABSTRACT

Liquefaction hazard mapping provides a useful tool for risk mitigation planning in seismic areas. Mapping for large areas is usually pursued by applying simplified criteria which rely on geological/lithological data and/or index properties of investigated soils, and in which local seismicity is not adequately considered (grade-1 methods). When a large number of in situ-tests and a reliable seismic hazard analysis are available, liquefaction hazard can be investigated by applying in-situ test-based methods accounting for seismic loading and the susceptibility of in-situ soil volumes (grade-2 methods). Advances in geotechnical earthquake engineering currently allow both deterministic and probabilistic evaluation of liquefaction potential by such methods. Liquefaction hazard can be parameterized concisely by a liquefaction potential index which expresses the liquefaction potential of investigated soil profiles. This paper provides a comparative case-study of liquefaction hazard mapping for a large coastal area in Central Italy, for which data from 1325 CPT soundings, covering an area of about 1300 km^2, are available. Two types of areal maps are produced. In the first type, zonation occurs solely through spatial interpolation of liquefaction potential index values. In the second case, zonation is performed on the basis of lithological, geological and seismic information. Hazard parameters are associated to each lithological-geological unit on the basis of statistical analyses yielding empirical cumulative distribution functions of the liquefaction potential index. Here, the two approaches to hazard mapping are implemented in the study area; their results are assessed and compared.

INTRODUCTION

In recent years, a growing interest in the effects induced by the seismic liquefaction on the built environment has taken place in Italy, as clearly indicated by the most recent provisions for building in seismic areas (EN-1998-5 2002, D.M. 14.01.2008). Consequently, several studies and research programs for liquefaction hazard zonation, even on a large scale, have been activated. These studies involve some of the most seismic areas in Italy such as the Gioia Tauro plain [Facciorusso & Vannucchi 2003], the Catania urban area [Crespellani et al., 2000], Nocera Scalo [Crespellani & Madiai, 2002] and the Romagna Adriatic Coast [Crespellani et al., 2003].

In general, seismic microzonation analyses, especially for large-scale areas (1:50.000 or greater), require simplified empirical methods to evaluate the liquefaction potential of a soil deposit, that is the magnitude of triggering risk of liquefaction phenomena due to an expected seismic event.
Such simplified criteria (grade-1 methods) rely on geological/lithological data and on the index properties of investigated soils, and, generally, do not adequately consider the local seismicity [TC4, 1999]. Nonetheless, they can be very helpful to delineate the critical areas requiring analyses at a more detailed scale. In such cases, more complex methods (grade-2 methods) are needed to evaluate liquefaction resistance of each layer of the soil deposit from in situ test results, and to compare it with the seismic demand quantified by local seismic hazard analyses. Such methods, even if they require more effort in terms of input parameters and calculation complexity, allow evaluation of the liquefaction potential of a soil deposit both horizontally and vertically. When the results of: (1) a large number of in situ-tests ; and (2) a regional seismic hazard analysis are available, grade-2 methods can also be applied over a large-scale area. An important issue concerns the concise spatial estimation and representation of liquefaction hazard from point values for the purpose of risk mitigation planning in seismic areas. When large areas are involved, the quality of spatial representations (i.e. maps) depends on additional factors such as the density and spatial homogeneity of data, the interpolation method and the reliability of the interpolated data.

CPT-BASED GRADE-2 METHODS: DETERMINISTIC AND PROBABILISTIC APPROACH

Grade-2 methods allow to compare the stresses induced on each layer of a soil deposit by an expected earthquake (triggering factor), to the soil critical stress state (susceptibility factor), which is expressed as a liquefaction resistance curve. The seismic demand is generally estimated, for a certain return period, T_R, by local seismic hazard analyses in terms of moment magnitude, M_W, and horizontal peak ground acceleration, a_{max}. The latter is obtained at the soil surface and eventually corrected with depth by a soil amplification factor. The liquefaction resistance curve is obtained by empirically correlating liquefaction (and non-liquefaction) observed field performance during the past seismic events (from which detailed and systematic observations are available) with soil properties, measured in situ and/or in the laboratory, that can be considered somehow representative of soil resistance to seismic liquefaction. In-situ testing methods include geotechnical routine tests or geophysical techniques for measuring parameters such as the number of blows, N_{SPT}, the tip cone resistance, q_c, and the sleeve friction, f_s or the shear wave velocity, V_S. For each database case history, the seismic demand induced at the site by the actual earthquake is then calculated at the same depth of the critical layer that experienced (or did not experience) liquefaction phenomena. Seismic action is expressed by the cyclic shear ratio (CSR) and plotted against the selected in situ test parameter. The latter is measured at the same depth, generally in post-seismic conditions, and opportunely corrected and normalized (Fig. 1). A discrimination curve between liquefaction and non-liquefaction cases is then traced visually or through more complex methods (e.g. using statistical regression). Such curve provides the resistance of soil to seismic liquefaction in terms of cyclic shear ratio (CRR) for each measured value of the selected soil parameter. This is traditionally known as the "deterministic approach". Since the 1970's, several empirical relationships have been developed for the most currently used in situ geotechnical tests. More recently, such relationships have been refined by the availability of larger data sets, comprising larger ranges of magnitudes of triggering events and more types of lithological and geological properties of the involved soil deposits. The increased data availability and ingenuous, innovative perspectives also allowed such relationships to be developed in a probabilistic form ("probabilistic approach").

Grade-2 methods are also known as "simplified" methods", since they require simplified boundary conditions (1-D analysis, free field, flat and horizontal ground level). Such methods are currently limited in their use (even if the estimated liquefaction potential is generally conservative).

As previously mentioned, advances in geotechnical earthquake engineering currently allow both deterministic and probabilistic evaluation of liquefaction potential by grade-2 methods.

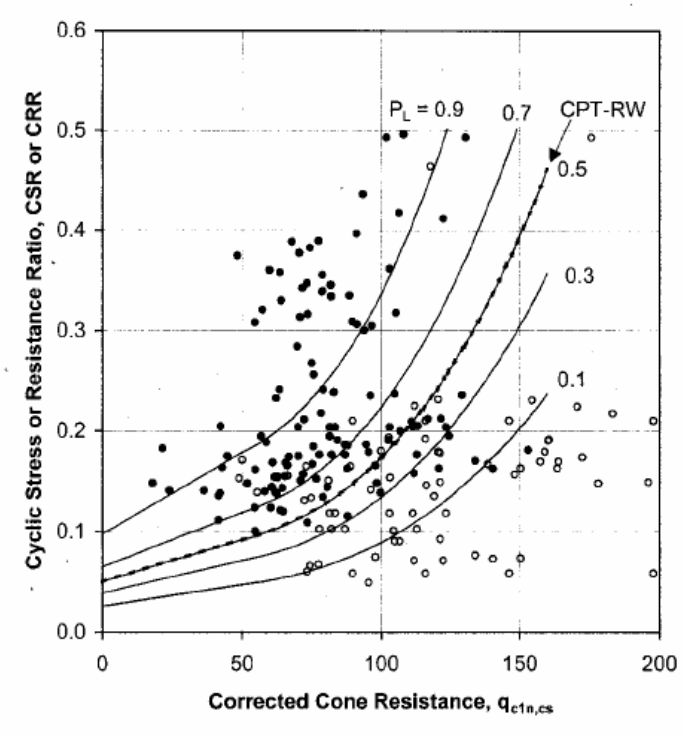

Fig. 1. Liquefaction triggering probability curves and deterministic liquefaction resistance curve [after Juang et al., 2002].

The first approach, more commonly used and scientifically more consolidated, generally implies the use of a deterministically and empirically estimated liquefaction soil resistance by the aforementioned relationships. The seismic demand is estimated empirically [Seed and Idriss, 1971]. The liquefaction potential is thus predicted in terms of safety factor (FSL), i.e. the ratio between the liquefaction soil resistance (CRR) and the seismic demand induced by the expected event (CSR). Liquefaction is expected to take place or not, if the calculated safety factory against liquefaction, FSL, is respectively lower or greater than a critical value (generally stated as 1, or greater than 1 if more conservatism is desired). The corresponding liquefaction potential, F(z), calculated at each depth and for each soil profile for which the in situ tests results are available, is set to "0" when FSL > 1 and to "1 – FSL", when FSL < 1.

The probabilistic approach, generally based on logistic regression models, (such as the maximum likelihood estimation models, the Bayesian updating method, the first-order reliability model or neural network-based methods), allows to simultaneously consider multiple descriptive variables than can influence the liquefaction soil resistance and to treat them as random variables. A liquefaction curve resistance is assigned to each value of the liquefaction triggering probability considered, P_L (Fig. 1). The liquefaction potential of each investigated layer induced by an expected reference earthquake is now expressed in terms of P_L [F(z) =

P_L] and is calculated from the liquefaction triggering probability curves (Fig. 1) once the expected seismic demand, CSR, has been estimated and the value of the selected soil parameter has been evaluated.

Although the deterministic approach provides simple and practical "formulae" to estimate liquefaction soil resistance and seismic demand, such relationships, even in the most refined form, have no formal probabilistic basis. Hence, they do not allow an explicit insight into the aleatory and epistemic uncertainties which are inherent to seismic liquefaction phenomena. On the other hand, the use of probabilistic tools allow to estimate and, in many cases reduce, relevant uncertainties regarding measurement and model errors, inherent variability of soil properties, etc. Readers are referred to Uzielli et al. [2007] for a state-of-the-art review of soil variability modeling in geotechnical engineering. Probability-based method are also more efficient in expressing the likelihood of initiation of liquefaction at a certain site as a "probabilistic quantity" related to an uncertainty level that can be usefully adopted in project-specific engineering evaluation of liquefaction soil resistance (i.e. land planning and mitigation risk of wide areas). Unfortunately, a probabilistic approach always requires the objective or subjective quantification of the uncertainties related to the relevant parameters and to the probabilistic model. Regarding the latter, most of the probabilistic models available in the literature to estimate the probability of liquefaction triggering still require significant calibration and validation.

LIQUEFACTION HAZARD MAPPING: SPATIAL INTERPOLATION AND STATISTIC-BASED CLASSIFICATION

Liquefaction hazard mapping can be better pursued by referring to an integral parameter (representative of each investigated soil profile) that concisely parameterizes the liquefaction potential of the profile itself. Such parameter is generally obtained through a cumulative sum of the liquefaction potential, F(z), estimated deterministically or probabilistically for each soil layer by means of one of the previously mentioned grade-2 methods. The "cumulative liquefaction potential" is generally extended to a depth (critical depth) where liquefaction-induced effects can be considered significant (15 ÷ 20 m). The parameter is weighted inversely with depth, i.e. weight progressively decreases with increasing depth.

With reference to a deterministic perspective, an expression for the cumulative liquefaction potential, better known as "liquefaction potential index", LPI, was proposed by Iwasaki et al. [1982] in terms of the safety factor, FSL:

$$LPI = \int_{z_{cr}}^{0} F(z) \cdot W(z) dz \qquad (1)$$

where z_{cr} is the critical depth, F(z) is the liquefaction potential and W(z) = 10 -1/2 z is the weighting function. The liquefaction potential index values range between 0 and 100 (if z_{cr} = 20 m). Such a scale does not have any inherent physical significance, and can only be related to the severity of liquefaction through calibration against real observations of seismically induced liquefaction effects (sand boils, lateral spreading, liquefaction flow, etc.) as proposed by Sonmez [2003] in Table 1.

When a probabilistic perspective is pursued, Eq. (1) can also be used to express the "cumulative liquefaction potential" in terms of triggering probability by setting F(z) = P_L,. A new liquefaction potential index, LPbI (named as liquefaction probability index, in the following) is so introduced to quantify the site liquefaction hazard [Facciorusso and Vannucchi, 2009]. In such case, liquefaction hazard is represented by an average liquefaction triggering probability weighted along the investigated soil profile. Hazard classes can be defined on the basis of the safety level to be guaranteed (see example in Table 2).

Once liquefaction hazard has been concisely parameterized for each investigated soil profile by the liquefaction potential index, LPI, or the liquefaction probability index, LPbI, hazard mapping is generally performed by means of spatial or geostatistical interpolation techniques. Interpolation criteria, data density and spatial variability can strongly influence the magnitude and reliability of interpolation outputs. Moreover, the spatial contouring of equi-hazard zones, being a product of a mathematical process, may not correspond to local seismicity areas and lithological composition of underlying soils, thereby resulting in "non sense" solutions, especially where few or low-quality data are available.

In this paper, an alternative approach of hazard mapping is proposed. Firstly, zonation is performed on the basis of lithological, geological and seismic information. In such an approach, hazard zones which can be considered homogeneous from a lithological and seismological point of view are preliminary contoured. Secondly, a hazard level, expressed in terms of exceedance probability of a threshold value of the liquefaction potential index, is then estimated for each zone. Such estimation requires statistical analysis of the LPI values distribution as well as the adoption of a probability model for the empirical probability density functions (pdf) and cumulative distribution functions (CDF).

Table 1. LPI-based hazard classes [Sonmez, 2003].

Liquefaction potential index, LPI	Liquefaction hazard
LPI = 0	Absent
0 < LPI≤ 2	Low
2 < LPI≤ 5	Moderate
5 < LPI≤ 15	High
LPI > 15	Very high

Table 2. *Liquefaction triggering probability classes [Chen e Juang, 2000]*

Class	Liquefaction triggering probability, P_L	
5	$P_L \geq 0.85$	Liquefaction almost certain
4	$0.65 \leq P_L < 0.85$	Liquefaction very probable
3	$0.35 \leq P_L < 0.65$	Liquefaction and non-liquefaction equally probable
2	$0.15 \leq P_L < 0.35$	Liquefaction improbable
1	$P_L < 0.15$	Non-liquefaction almost certain

AN ITALIAN CASE-STUDY: THE COSTAL AREA OF THE EMILIA-ROMAGNA REGION

Geological, Lithological and Seismological Settings

The selected case-study covers a large coastal area in Central Italian region of Emilia Romagna. The area has been subjected to an extensive geological and geotechnical survey in the past years. Many research programs have been activated by the Regional Government to locally assess the liquefaction hazard [Marcellini et al., 1998, Cipriani et al., 2000, Crespellani et al., 2003]. These studies are concordant in confirming the susceptibility of some soil deposits along the coastal area to liquefaction as suggested by historical chronicles from the past strong earthquakes [Galli and Meloni, 1993]. A high vulnerability due to the economical and industrial relevance of some harbor infrastructures (e.g., Rimini and Ravenna), a high population density, an invaluable heritage (e.g., the historical centre of Rimini) are important contributors to the high liquefaction risk in the area. Liquefaction hazard mapping addressed an area of about 1300 km^2, located between the Adriatic Coast and the inner Apennine edge and including the coastal municipalities located between Milano Marittima and Misano Adriatico (Fig. 2). Morphologically, the area consists prevalently of a low plain valley, with a few hilly formations in the Southern edge, and a densely populated, narrow coastal strip (around 800-1000 m in width for a length of about 100 km), mostly comprising sea coastal deposits and Aeolian dunes.

A very large database comprising more than 3700 CPT soundings and 1800 boreholes has been collected in the past years by the regional and local governments. A reduced dataset was identified for this study by only including the CPT test results which could have been considered reliable and with maximum explored depths greater than 15 m (at which liquefaction effects are deemed to be relevant). Such dataset includes data from 1325 CPT soundings: prevalently mechanical (1082) and, for the remaining part (243), electrical, piezocone (CPTU) or seismic piezocone (SCPTU). The maximum sounding depth exceeds 30 m in 330 of the selected CPT's (25.4%). Water table measurements are available for 797 CPT's (58.3%). In the remaining soundings, the groundwater level was estimated by adopting interpolation criteria, and expected to vary approximately between 1.5 m e 2 m from ground surface. The CPT soundings cover quite uniformly the whole studied area (with an average density of about 1.1 CPT/km^2), with the exception of a limited zone in the Northern part (Comacchio Valleys), where only a few data are available, as shown in Fig. 2. The maximum data density (of about 15 CPT/km^2) is reached on a narrow strip of the coastal area at less than 1 km of distance from the shore line.

The lithological units which characterize the most recent and outcropping deposits are depicted in Fig. 2, along with the locations of CPT soundings. From a lithological point of view, the area can be subdivided into three main stripes extending from NW to SO direction, i.e. parallel to the coast. The first stripe, proceeding inland from the coast, has an average width of about 1 km in the Central and Southern part, and is prevalently composed of coastal well-graded medium, fine and finest sands (shore sands and Aeolian dunes) with a maximum thickness ranging between 8 m and 12 m. In the Northern part, where its width is slightly greater, it consists of sandy clays of coastal plain.

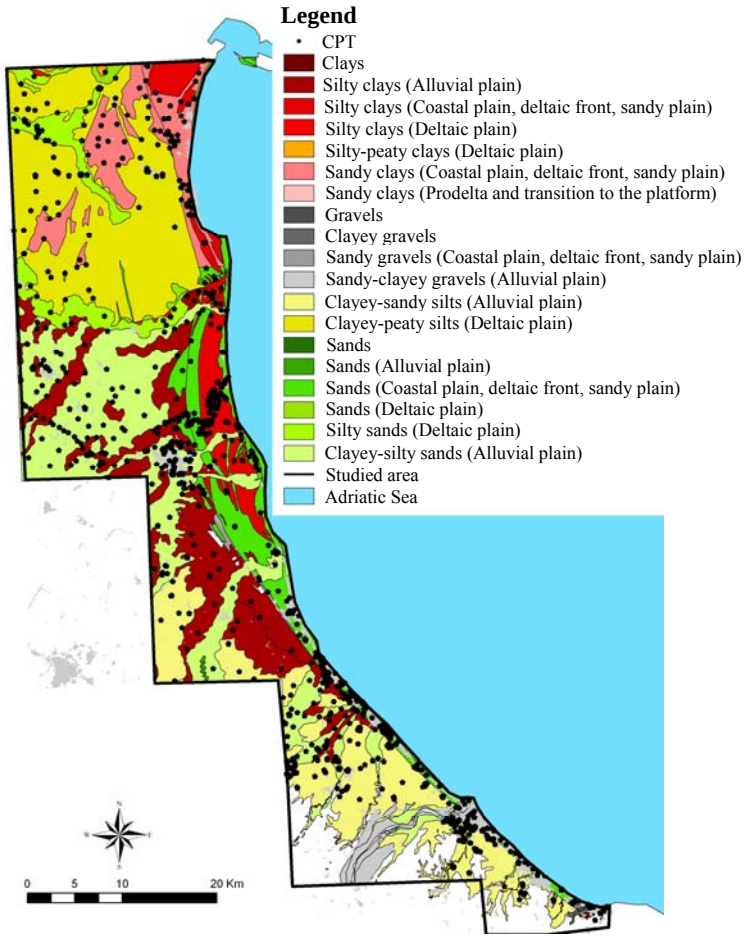

Fig. 2. Map of lithological units and selected CPT's.

A different composition and sedimentary origin characterize the underlying deposits of the intermediate strip: clayey-peaty silts of deltaic plain in the Northern part, of larger width, and alluvial sandy-clayey deposits in the Southern part. Such intra-valley fluvial and alluvial plain deposits of Middle Pleistocene – Holocene age often alternate with shore sands levels. Their thickness increases from the inner Apennine margin to the Adriatic coast and reaches a maximum value of about 20 – 25 m in the Southern part, but does not exceed 10 m in the Central and Northern areas. The third and inner stripe is of little interest from a liquefaction point of view as it consists prevalently of outcropping rock in the Southern part and of silty clay and silty-clayey sands of alluvial origin in the Central part. Organic clays, silts, sands and gravels of alluvial origin are present in the older deposits that can be encountered under the first 10 – 20 m of soil, with shore sand intercalations in proximity of the coast.

An expected seismic event for a selected return period, T_R, must be defined preliminarily to calculate the seismic demand. The horizontal peak ground acceleration, a_{max} and the moment magnitude, M_w, are sufficient to characterize the expected earthquake when a simplified method is used. Such parameters can be completely defined for each sounding once a reliable local seismic hazard analysis has been performed and the seismic response of the soil deposits overlying the bedrock has been estimated. More precisely, the horizontal peak ground acceleration a_{max} can be obtained by applying the following equation:

$$a_{max} = a_g \times S_S \times S_T \quad (2)$$

where a_g is the expected horizontal peak acceleration on firm soil in free field condition. Such parameter is generally deduced together with the moment magnitude, M_w, from local seismic hazard analyses, when available. S_S is the stratigraphic amplification factor, which accounts for changes in the seismic excitation through the layers of the soil deposit. This parameter can be estimated from a local seismic response analysis whenever possible, or through empirical relationships, as shown below. S_T is the topographical amplification factor. In the following, S_T will be assumed to be equal to one, since flat conditions are prevailing in the considered area.

The reference return period, $T_R = 475$ years, is provided by the Italian seismic building provisions [D.M. 14.01.2008] for a selected safety level ("Limit state of safeguard") and for ordinary buildings (50 years of lifetime) together with the firm soil peak horizontal acceleration values, a_g, which are defined for each node of a national reference grid from a base seismic hazard analysis. A four-node weighted average is then calculated for each CPT location; the corresponding a_g values range from 0.07 g to 0.19 g, with the highest values in the Central and Southern parts of the case-study area. Since it was not possible to perform a seismic response analysis for each of the selected 1325 sites, once again the National seismic provisions were adopted to estimate the amplification factor S_S. The latter depends on the seismic hazard parameters previously adopted and on the soil class which can be assigned to the first 30 m of soils on the basis of the stratigraphic composition of the soil deposit and the equivalent shear wave velocity, V_{S30}. When a direct measure of V_S was not available, V_{S30} was estimated from the CPT results through empirical relationships [Giretti et al., 2007]. The worst-case soil profile (class D) was assumed when the maximum explored depth resulted lower than 30 m. The estimated S_S values are rather uniformly high in the entire studied area, ranging between 1.7 and 1.8, with the lowest values in the Central part.

Two different procedures were implemented to evaluate the expected moment magnitude, M_W, for a 475-year return period: (1) a seismogenetic-based criterion, where the strongest earthquake is considered in a period of 475 years within the same seismogenetic zone [INGV, 2004], where the probability of earthquake occurrence is uniformly distributed; and (2) a disaggregation-based criterion, which allows to estimate the magnitude and epicentral distance of the most hazardous event for the site [INGV, 2007]. By taking the maximum value obtained by the aforementioned procedures, two regions of uniform M_W values were then identified. These are shown in Fig. 5: the first region covers the Central part of the investigated area, where the expected magnitude is 5.9 (and which entirely falls within the ZS9 seismogenetic zone); the second region, with the maximum expected magnitude of 6.0, lies in the Southern sector of the study area, within the ZS12 seismogenetic zone. The remaining part of the study area does not fall within any seismogenetic zone. For such an area, the expected magnitudes, ranging between 5.0 and 5.3, were estimated by disaggregation of the seismic hazard data.

In conclusion, the case study area falls within a low-to-medium-seismicity zone where the expected magnitude ranges between 5.0 and 6.0 and the expected horizontal peak ground acceleration values, a_{max}, provided by the Equation (2), are quite variable, gradually increasing from moderate values (0.127 g) in the Northern part to extremely high values (0.335 g) in the Southern part.

Liquefaction Potential Evaluation

The Robertson and Wride method was chosen in this study among CPT-based simplified methods to deterministically evaluate the liquefaction resistance in terms of Cyclic Resistance Ratio (CRR) owing to its diffuse and long-time application in engineering practice, to its attractive form and simplicity. Herein, it is applied in a modified form by adopting the NCEER recommendation [Youd et al., 2001], also concerning the expected seismic demand. Further changes are also introduced in the formulation of the safety factor, FSL, and of the corresponding liquefaction potential expression, F(z).

Traditionally, the FSL value which discriminates expectation of liquefaction from non-liquefaction, and which accounts for the uncertainties introduced by the measured parameters (e.g.,

q_c, f_s,) and the adopted model, is assumed as unity. Nonetheless, a different conservative value can be established by the user, especially when high safety levels must be guaranteed in risk-based design. In the present paper, since the Building Seismic Safety Council (1994) recommends the Class 2 of liquefaction triggering probability (Table 2) for ordinary structures, a discrimination value of 1.4 was adopted. The selected value also accounted for the fact, demonstrated by Juang et al. [2002], that the Robertson and Wride method is non conservative (as better explained in Fig.1) and the recommended liquefaction triggering probability (e.g., P_L = 0.25) can be obtained with a discriminator value of FSL greater than one (e.g., FSL = 1.4), as explained in greater detail hereinafter. The aforementioned liquefaction potential function F(z) proposed by Iwasaki et al. [1982] is thus accordingly modified as suggested by Sonmez [2003]:

$$F(z) = \begin{cases} 0 & \text{if} \quad FSL > 1.4 \\ 2 \cdot 10^6 e^{-18.427 \cdot FSL} & \text{if} \quad 0.95 < FSL \le 1.4 \\ 1 - FSL & \text{if} \quad FSL \le 0.95 \end{cases} \quad (3)$$

As far as the probabilistic approach is concerned, several tools have been proposed in recent years to mathematically express the liquefaction triggering probability, P_L, that is the liquefaction potential $F(z) = P_L$. These are generally based on logistic regression models. Several methods [Moss, 2003, Juang et al., 2006] when tested on the CPT database used in this paper, produced large differences in calculation results and considerable divergences from the more consolidated deterministic methods in terms of normalization criteria of the cone tip resistance (i.e. the adjustment for fines content, corrections for effective overburden stresses), the influence of local seismic response on the seismic demand evaluation and the magnitude-corrected weighting factor. Moreover, a controversial issue is related to the COV (Coefficient of variation) values adopted to quantify the uncertainties regarding measurement errors, model imperfection and the inherent variability of soil properties. In order to obtain comparable deterministic and probabilistic liquefaction hazard maps, the probabilistic method proposed by Juang et al. [2002] was adopted in this paper. Such method, which relies on a Bayesian approach, allows to consider the same database used in the Robertson and Wride method and to treat its parameters as random variables (with normal distributions arbitrarily assumed). A reliability analysis is performed on the dataset by applying the First Order Reliability Method (FORM): the reliability index value, β, is calculated with respect to the limit state curve proposed by Robertson and Wride and associated with each case history data. Through Bayes' theorem, a Bayesian mapping function that relates the liquefaction triggering probability, P_L, to the reliability index, β, is constructed. To facilitate the application of such method, an equivalent mapping function which directly relates P_L to the safety factor FSL, estimated by the Robertson and Wride method, was also proposed by Juang et al. [2002]:

$$P_L = \frac{1}{1 + \left(\frac{FSL}{A} \right)^B} \quad \text{.....(4)}$$

where A = 1.0 and B=3.3. Such function is referred to herein.

LIQUEFACTION HAZARD AND PROBABILITY MAPPING

Spatial Interpolation

Once the liquefaction potential has been weighted and integrated [Eq. (1)] for each sounding over the same depth interval (1 ÷ 15 m), the obtained cumulative values, LPI or LPbI, must be interpolated for preset spatial locations in the case-study area and classified upon the aforementioned hazard classes, respectively listed in Tables 1 and 2, to contour the corresponding liquefaction hazard zones. A GIS software was used to manage the large spatially referenced dataset and to interpolate the calculated LPI and LPbI values. Several criteria for spatial interpolation are available. These are all based on mathematical processes which do not consider explicitly any statistical measure of the spatial randomness of the considered dataset, nor do they provide any reliability measure of the interpolated datum.

In this paper, the inverse weighted distance method is applied. Such method overlaps to the selected area a grid of nodes where the interpolation is performed by considering a weighted average of the closest surrounding data values. The weighting function is generally a power function, inversely related to the distance. The closest surrounding data values can be identified by taking the closest values in a predefined distance (circle radius criterion) or a preset number of data points. Some parameters must be arbitrarily selected. These include: the mesh size of the interpolating grid, L, which value is related to the size of the studied area and to the density of the dataset; the power index of the weighting function, n, which defines how rapidly the influence of the closest points can decrease with distance; and the selection criteria (and the corresponding parameters) of the closest data points to weight for interpolation, which can strongly influence the final aspect of the hazard map. When the interpolation relies on the same number of data points, each grid node returns an interpolated value, even if such value can be conditioned by spatially very distant data points, so that it may not reflect the real spatial behavior of the interpolating variable. When the circle radius criterion is adopted with a small value for the radius, R, the spatial heterogeneity of the dataset can be better considered and only the closest data points (more likely pertaining to the same lithological and seismological pattern) are allowed to influence the interpolated value. In such case, no interpolated values are provided for those nodes falling within an area where no data or not enough data are available. Even if the resulting hazard map, may appear chaotic and display a spatially irregular sequence of hazard classes, it is effective in revealing: (a) the spatial locations where no reliable hazard

values can be provided and where, consequently, it would be advisable to acquire additional data; and (b) those areas where the interpolation is strongly influenced by a single outlier value and the estimated liquefaction hazard cannot be confidently accepted. Such information allows a qualitative assessment of the reliability of the hazard map, even in absence of quantitative values.

In this study, a power index n = 2 and a mesh grid length L = 200 m were adopted. The circle radius criterion was applied with an influence distance R = 3500 m, which was deemed a good compromise between what is considered as the horizontal fluctuation distance for LPI [Lenz and Baise, 2007] and the minimum distance required to minimize the likelihood of occurrence of "no data" areas in the map. The hazard maps obtained in terms of liquefaction hazard and liquefaction triggering probability are reported, respectively, in Fig. 3 and Fig. 4. Hazard and probability classes contouring is performed with reference to the categories reported in Table 1 and 2, respectively. Figure 3 reveals prevailing low or absent liquefaction hazard in the case study area, and moderate and high hazard along a narrow strip of about 1 km wide of the Adriatic coast (from Cervia to Cesenatico and Rimini) and, locally, in some of the inner alluvial valleys (for example, between the historical centre and the harbor area of Ravenna).

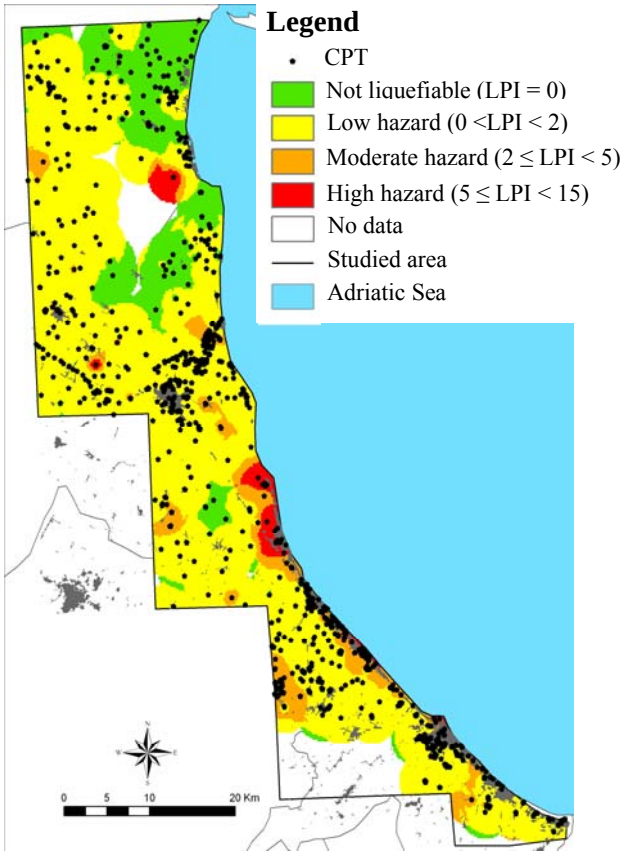

Fig. 3. Liquefaction hazard map of investigated area as obtained by spatial interpolation of calculated values of LPI.

There is a rather large zone in the Northern-Central part of the investigated area, and locally in some part of the inlands areas, where reliable spatial interpolation could not be performed due to insufficient or low-quality data. In such areas, either the liquefaction hazard is not quantified (white areas), or hazard values are determined by a single data point (sometimes an outlier). In the latter case, the corresponding hazard zones are of circular shape, as shown in Fig. 3. If liquefaction hazard is expressed in terms of liquefaction triggering probability, liquefaction hazard can be correspondingly considered negligible for the greater part of the case study area, where P_L is lower than 15% (non-liquefaction almost certain), and, only locally, along the Central and Southern Adriatic coast, it may become greater than 15%. (liquefaction improbable) or 35 % (liquefaction and non-liquefaction equally probable). As in the deterministic case, liquefaction hazard cannot be correctly estimated for a certain part of the investigated area.

Statistical-probabilistic Assessment of the Correspondence between Geological Features and Liquefaction Susceptibility

In the spatial mapping of soil properties, geological and lithological data are generally classified into compositionally and/or morphologically homogeneous units.

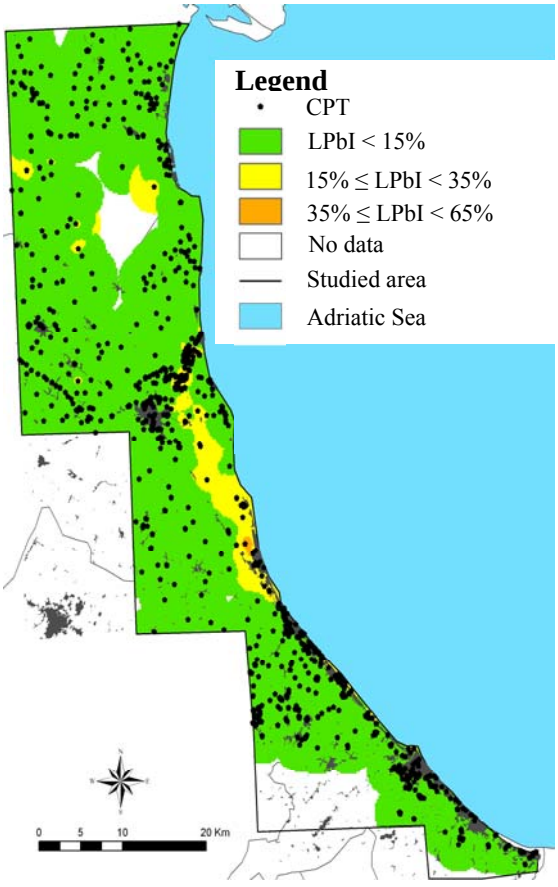

Fig. 4. Liquefaction probability map of investigated area as obtained by spatial interpolation of calculated values of LPbI.

It is well known that the correspondence (for engineering purposes) between compositional and mechanical soil properties is not univocal due to the complexity of in-situ conditions. Here, it is of interest to assess quantitatively the correspondence between geologic/lithological unit and CPT-based liquefaction susceptibility as parameterized by the LPI previously calculated. A statistical-probabilistic approach could effectively quantify the degree of correspondence (or lack thereof). In particular, with reference to the study area, the following issues could be addressed: (1) does liquefaction susceptibility differ significantly among different geological units?; and (2) does liquefaction susceptibility vary significantly inside the same geological unit? A three-step approach was implemented: first, a preliminary zonation, based on the natural boundaries of the lithological units of the outcropping layers (as illustrated in Fig. 1) and on local seismicity, was performed. For sake of simplicity, the lithological units, listed in the legend of Fig.1, were grouped by geological origin, i.e., sedimentary conditions and depositional processes (coastal or alluvial), and lithological properties (sands, gravels, silts and clays) into six main groups, described in Table 3. Within each lithological unit, seismically homogeneous sub-units (i.e. with the same magnitude of triggering factors) were subsequently defined with regard to local seismicity.

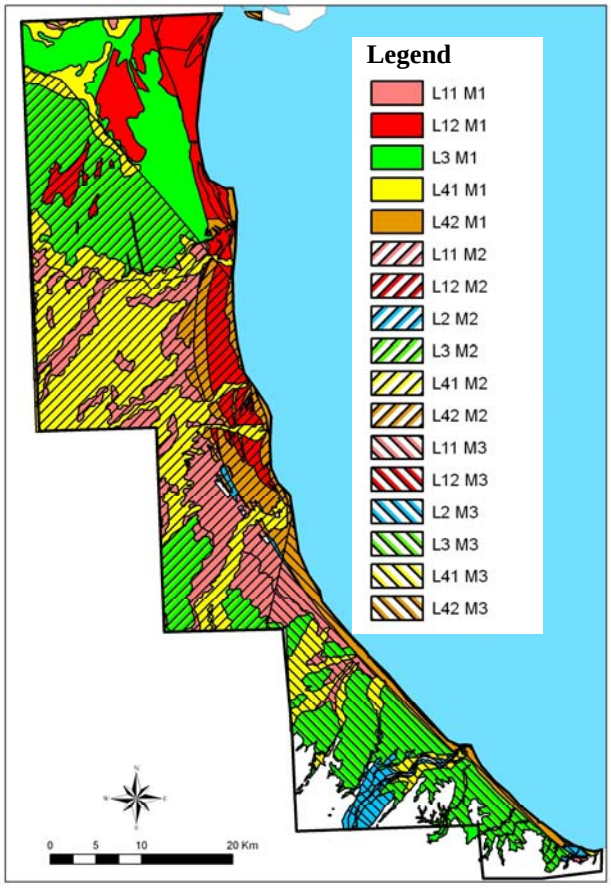

Fig. 5. Map of equi-hazard zones described in Tab.3.

Three moment magnitude-related classes were identified on the basis of the expected magnitude classification previously described: M1 (for $M_W < 5.3$); M2 ($M_W = 5.9$) and M3 ($M_W = 6.0$). The parameter a_{max} was not considered as triggering parameter since it displayed limited variation among the identified classes, with the standard deviation ranging between 0.02 and 0.18. A total of sixteen hazard zones, coded according to lithological unit and magnitude class (L# M#), were identified. These are described in Table 3 and illustrated in Fig. 5. In principle, if the correspondence between compositional and mechanical properties of soils is strong, it may be expected that the cumulative liquefaction potential are comparable within the same zone.

In the second step of the procedure, relative frequency histograms of LPI were obtained for each hazard zone. The empirical histograms are shown in Fig. 6, with some important statistics (i.e. numerosity, N, mean, standard deviation, St.Dev., and coefficient of variation, COV).

The frequency histograms were found to be strongly asymmetric and skewed. In some cases, either not enough data were available or the LPI variance was judged to be too high to formulate any reliable statistical inference about the behavior of LPI within the same hazard zone. Such cases (defined quantitatively on the basis of the criterion: $COV/\sqrt{N} > 0.35$ or $N < 30$) were not analyzed further and are coded as "NA/NG" in Tab.3.

Thirdly, a hazard level, expressed in terms of the probability of exceedance of one or more preset threshold values of the LPI, was calculated for each zone. Such calculation was pursued through the selection and fitting of suitable probability models to the previously calculated relative frequency histograms. The shape and the skewness of the empirical histograms suggested the adoption of an exponential model for all 16 zones. The empirical CDF's (bar diagrams) and the fitted exponential CDF's (solid lines) are reported in Fig. 7 with the lower and the upper bounds of the 95% confidence interval (dashed lines). Cumulative values were also expressed in a complementary form (1-CDF) and compared with the threshold values of LPI (black solid lines) to explicit the respective probabilities of exceedance for each hazard zone, as shown in Fig. 8.

Two reference threshold values were considered: LPI = 5, which corresponds to the assumed higher-bound safety level as suggested by Toprak e Holzer [2006], and LPI = 2 which corresponds to the lower-bound safety level, as suggested by the new hazard classification of Table 1. The probabilities of exceedance of the two reference values (PL_5 and PL_2, respectively) are listed in Table 3 along with the mean values of LPI, the standard deviations and the corresponding hazard classes, as proposed by Sonmez [2003]. Fig. 8 shows the result of such analysis for the deterministic liquefaction potential LPI.

The following observations can be drawn from the results:

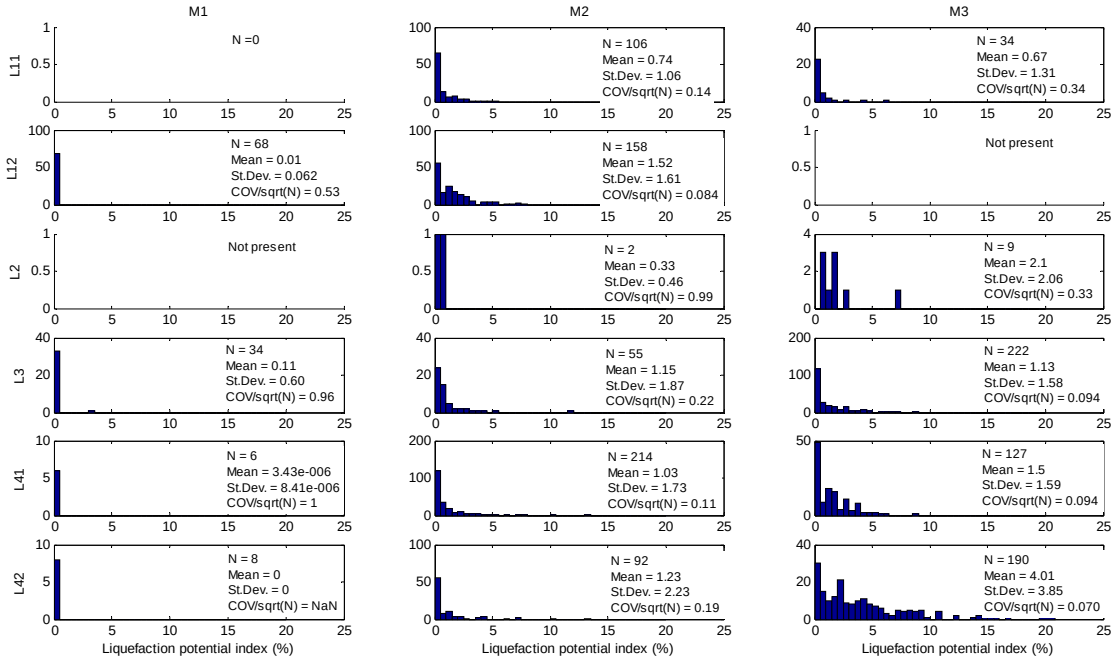

Fig. 6. LPI empirical frequency histograms of LPI values.

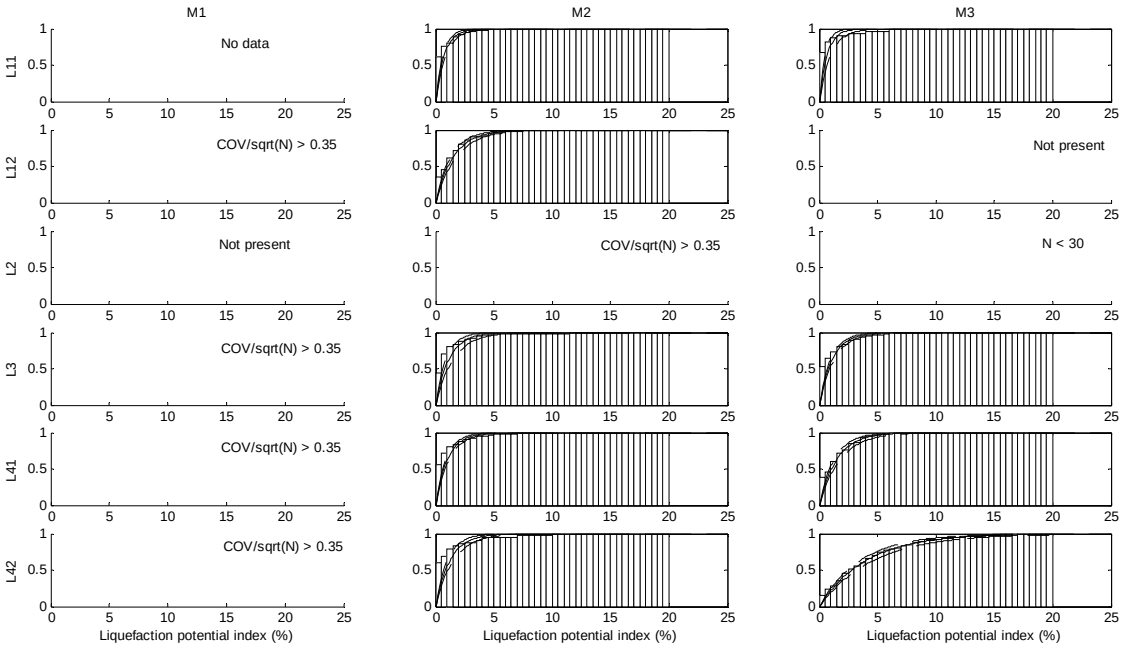

Fig. 7. Empirical and theoretical (exponential) CDF's of LPI values.

- the equi-hazard zones for which not enough or poor quality data were available (NA/NG) actually account for a small fraction (less than 2%) of the area of interest (L11 M1, L2 M2 and L42 M1) or they correspond to regions of scarce interest for liquefaction, such as the hilly southern-inner part with prevalently outcropping rock (L2 M3). On the contrary, zones L12 M1, L3 M1 and L41 M1 cover a large part of the lowest-magnitude region ($M_W < 5.3$). Hence, even if the statistical approach could not be applied because only a few data were available and almost uniformly centered around zero (as shown in Fig. 6), the probability of liquefaction triggering and the LPI mean values can be reasonably supposed equal to zero in such areas;
- the lower values of the exceedance probabilities (low liquefaction hazard) refer to the alluvial clays, while intermediate values (low-to moderate liquefaction hazard) are typical of the coastal clays, silts and alluvial sands; the greatest exceedance probabilities

occurred for the coastal sands (PL_2 = 60% and PL_5 = 28.8%), as expected;
- the magnitude class (M1, M2 or M3) seems to influence the liquefaction hazard parameters only for particularly susceptible soils (L42).

The proposed approach relies on the important assumption that the horizontal and vertical variability of soil properties relevant for liquefaction susceptibility (susceptibility factors) and of the seismic parameters of the expected earthquake (triggering factor) are limited within each hazard zone. Such assumption seems to be confirmed "a posteriori" by the small variances of calculated LPI values. Nonetheless, a further confirmation was sought by explicitly addressing soil type based on available borehole data. Soil stratigraphies from 1800 boreholes were used to assess the continuity and homogeneity of the outcropping lithological units (which were used to define the hazard zones preliminarily) in the underlying 10÷15 m of soil deposit. Stratigraphic logs were discretized at 1-metre intervals; soil type descriptions were associated to each discrete layer using the same soil type index number previously used for hazard classification (see Table 3), i.e., 1 = clays; 2 = gravels; 3 = silts; 4 = sands; 5 = organic soils. For each 1 meter-thick layer, the relative frequency histogram of soil type index, normalized by the modal relative frequency value (i.e. the maximum relative frequency value) was estimated within the same hazard zone. The results of the above calculations are reported graphically in Fig. 9. The figure allows appreciation of the shape of the normalized frequency of soil type with depth. In particular, it is possible to appreciate the depth-wise prevalent soil type as well as the compositional heterogeneity (represented by the scatter in soil type index values). The analysis reveals the soil deposits can be assumed quite homogeneous with depth for L3, L41 and L42 hazard zones: silty and sandy layers (respectively) can be encountered more or less continuously in the first 10÷15 m of soil deposit for such lithological units. For lithological units L1 and L2, though silty and sandy layers seem to prevail especially in the deeper layers, these seem to have no influence on liquefaction potential, as demonstrated by the previously calculated LPI values.

FINAL REMARKS

In the present paper, a case-study of liquefaction hazard mapping is presented for a large coastal area of about 1300 km^2 in Central Italy, where data from 1325 CPT soundings covering an area are available. CPT-based grade 2 methods are applied to estimate the liquefaction potential of soil deposits, both deterministically and probabilistically. A cumulative index (LPI) which concisely parameterizes the liquefaction potential of sounded soils in terms of safety factor, FSL, or liquefaction triggering probability, PL, was defined and used for liquefaction hazard mapping. Two types of areal maps were produced.

In the first type, zonation of liquefaction hazard relies solely on spatial interpolation of cumulative liquefaction potential values, with no preliminary categorization performed.

Table 3. Probability of exceedance of reference threshold values, LPI mean values (± standard deviation) by hazard zone.

Hazard zones		LPI	PL_2	PL_5
Lithology	Seismicity			
L11-Alluvial Clays (clays, silty clays of alluvial or deltaic plane)	M1*	NA/NG[+]	-	-
	M2**	0.7±1.1 (low)	6.6	1.1
	M3***	0.7±1.3 (low)	5.0	0.1
L12-Coastal Clays (silty and sandy clays of coastal origin)	M1	NA/NG	-	-
	M2	1.5±1.6 (low/moderate)	26.9	3.7
	M3	NP[++]	-	-
L2-Gravels (Clayey and sandy gravels of coastal and alluvial origin)	M1	NP[++]	-	-
	M2	NA/NG	-	-
	M3	NA/NG	-	-
L3-Silts (Clayey and sandy silts of alluvial and deltaic origin)	M1	NA/NG	-	-
	M2	1.2±1.9 (low/moderate)	17.4	1.3
	M3	1.1±1.6 (low/moderate)	16.9	1.2
L41-Alluvial Sands (Sands, sitly and clayey sands od alluvial and deltaic origin)	M1	NA/NG	-	-
	M2	1.0±1.7 (low/moderate)	14.2	0.8
	M3	1.5±1.6 (low/moderate)	26.4	3.6
L42- Coastal sands (Coastal sands)	M1	NA/NG	-	-
	M2	1.2±2.2 (low/moderate)	19.7	1.7
	M3	4.0±3.9 (moderate/high)	60.8	28.8

* M_W < 5.3, ** M_W =5.9; ***M_W = 6.0; [++] Not present
[+] NA/NG=insufficient or unreliable data

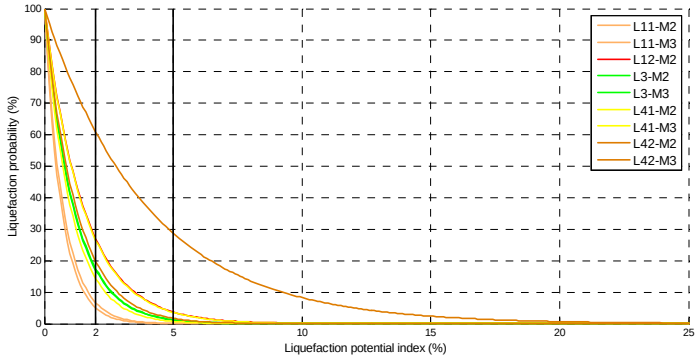

Fig. 8. Exceedance probability of the threshold values of LPI.

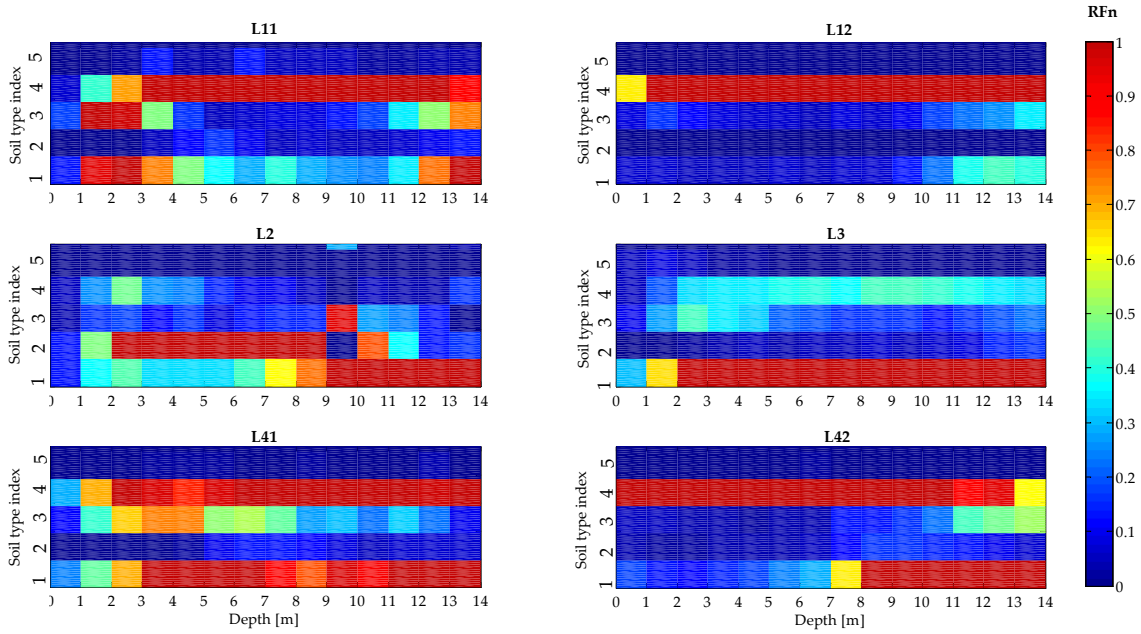

Fig. 9. Normalized relative frequency (RF_n) histograms of soil type index for discretized sounded profiles from 1800 boreholes, by lithological units.

An inverse distance weighted method was applied. In this type of map, liquefaction hazard zones typically display irregular and apparently erratic spatial patterns due to the inherent variability of soil properties and triggering factors. Even if the reliability of the interpolated data is non explicitly considered, it may be qualitatively estimated by opportunely setting the interpolation criterion and parameters.

In the second type of mapping, a preliminary zonation was performed on the basis of lithological units and of the (spatially variable) expectable seismicity. Sixteen zones where lithological properties (at least in the surficial layers), and seismic triggering factors (primarily in terms of moment magnitude and secondarily in terms of peak ground acceleration) could be considered to be uniform, were identified. The previously calculated values of LPI were analyzed statistically and spatially referenced by hazard zone. Zone-specific statistical properties of LPI values were obtained in the form of relative frequency histograms and empirical cumulative distribution functions. Exponential probability model were fitted to the cumulative distribution functions. Probabilities of exceedance of present threshold values for LPI (relevant for engineering purposes) were derived.

Comparison of the two map types allows several interesting observations and assessments to be made. First, each map type displays advantages and disadvantages over the other. For instance, when compared with those obtained by spatial interpolation, the liquefaction hazard parameters obtained by preliminary zonation (i.e., PL_2, PL_5 or mean(LPI) ± st.dev.) reveal a more continuous, smoother spatial behavior, with more regular and detectable liquefaction hazard zones. On the other hand, the upper-bound values of hazard from preliminary zonation are generally lower since they are the results of spatial averaging over wide areas. Hence, with increasing size of homogeneous lithological-seismic hazard zones, there is a decrease in conservatism which could

potentially lead to undesirable underestimation of hazard. A loss of resolution also occurs. With reference to the illustrated case-study, both types of mapping confirmed that the high-hazard area for seismic liquefaction is limited to the Central and Southern coastal region, and that liquefaction hazard can be generally assumed to be low or locally moderate in the remaining spatial locations.

REFERENCES

Building Seismic Safety Council, [1994]. *"NEHRP recommended provisions for seismic regulations for new buildings"*. Federal Emergency Management Agency.

Chen, C.J. and C.H. Juang, [2000]. "Calibration of SPT- and CPT-based liquefaction evaluation methods." Innovations Applications in *Geotechnical Site Characterization*, Mayne, P. and Hryciw, R., Eds., Geotechnical Special Publication No. 97, ASCE, New York, pp. 49−64.

Cipriani S., T. Crespellani, C. Madiai, D. Pierucci, G. Vannucchi, A. Marcellini, L. Martelli and G. Frassineti [2000]. "Carta del rischio di liquefazione in un'area ricca di beni culturali: la costiera romagnola." *Atti del Covegno "Condizionamenti geologici e geotecnici nella conservazione del patrimonio storico culturale"*. Torino.

Crespellani, T., E. Cascone, F. Castelli, S. Grasso, M. Maugeri and G. Vannucchi [2000]. "Liquefaction potential of saturated sand deposits in the urban area of Catania". In E. Faccioli and V. Pessina (Eds), *The Catania Project: earthquake damage scenarios for high risk area in the Mediterranean*, CNR - GNDT. Roma. pp. 46-51, ISBN 88-900449-0-X.

Crespellani, T. and C. Madiai [2002]. "Liquefaction risk analysis during earthquakes at Nocera Scalo, Italy, Part II: total and effective stress-strain analyses for liquefaction prediction". Italian Geotechnical Journal, N.4, pp. 46-65.

Crespellani, T., C. Madiai and G. Vannucchi [2003]. "CPT-based liquefaction hazard maps for an Italian coastal area". Italian Geotechnical Journal, N. 4, pp. 46-65.

D.M. 14.01.2008. *"Decreto Ministeriale del 14/01/2008. Norme Tecniche per le Costruzioni"*.

(pr)EN 1998‑5 [2002] *"Foundations, retaining structures and geotechnical aspects"*. CEN European Committee for Standardization, Bruxelles, Belgium.

Facciorusso, J. and G. Vannucchi [2003]. "Application of geostatistical methods to the definition of a liquefaction hazard map for the harbour area of Gioia Tauro". *Proc. Fourth Int. Conference on Seismology and Earthquake Engineering*, Tehran, Iran.

Facciorusso, J. and G. Vannucchi [2009]. An Italian Example Of Large-Scale Regional Mapping Of Liquefaction Potential: Deterministic And Probabilistic Approach. Italian Geotechical Journal, Vol. 2/09, pp. 34-57.

Galli P. and F. Meloni [1993]. *"Nuovo catalogo nazionale dei processi di liquefazione avvenuti in occasione dei terremoti storici in Italia"*. Il Quaternario, 6 (2), Gruppo di lavoro CPTI (2004). Catalogo Parametrico dei Terremoti Italiani, versione 2004 (CTI04), INGV, Bologna, pp. 271-292.

Giretti, D., A. Colombi and V. Fioravante [2007]. "Sulla valutazione della velocità di propagazione delle onde di taglio da prove penetrometriche statiche per i depositi alluvionali ferraresi". Rivista Italiana di Geotecnica, Vol. 3/07, pp 48-59.

Istituto Nazionale di Geofisica e Vulcanologia (INGV) - Gruppo Di Lavoro Per La Redazione Della Mappa Di Pericolosità Sismica, Ordinanza PCM 20.03.03 n.3274 [2004]. "*Zonazione sismogenetica ZS9*", INGV, Bologna.

Istituto Nazionale di Geofisica e Vulcanologia (INGV) - Dipartimento della Protezione Civile (DPC) [2007]. *"Deliverable D14. Disaggregazione della pericolosità sismica in termini di M-R-e"*.

Iwasaki, T., K. Tokida, F. Tatsuoka, S. Watanabe, S Yasuda and H. Sato [1982]. "Microzonation for soil liquefaction potential using simplified methods". In: *Proceedings of 3rd Int. Conf. on Microzonation*, Seattle, Vol 3. pp 1319–1330.

Juang, C.H., T. Jiang, T. and R.D. Andrus [2002]. "Assessing probability-based methods for liquefaction evaluation". Journ. of Geot. and Geoenv. Eng., ASCE, 128(7), pp. 580−589.

Juang C.H., S.Y. Fanf and E.H. Khor [2006]. "First-order reliability method for probabilistic liquefaction triggering analysis using CPT". Journ. of Geot. and Geoenv., ASCE, 132(3), pp. 337−350.

Lenz J. and L.G. Baise [2007]. "Spatial variability of liquefaction potential in regional mapping using CPT and SPT data". Soil Dyn. and Earth. Engin., 27 (7), pp. 690-702.

Marcellini A., R. Daminelli, M. Pagani, F. Riva, T. Crespellani, C. Madiai, G. Vannucchi, G. Frassineti, L. Martelli, D. Palombo and G. Viel [1998]. "Seismic microzonation of some Municipalities of the Rubicone area (Emilia-Romagna region." *Proc. of the Eleven11th European Conf. on Earthquake Eng.*, Paris, Balkema, pp. 339- 350.

Moss R.E.S. [2003]. "*CPT-based probabilistic assessment of seismic soil liquefaction initiation"*. Ph.D. Dissertation, Univ. of California, Berkeley, Calif.

Seed, H. B. and Idriss, I. M. [1971]. ''Simplified procedure for evaluating soil liquefaction potential.'' J. Geotech. Engrg. Div., ASCE, 97(9), pp. 1249–1273.

Sonmez H. [2003]. “Modification to the liquefaction potential index and liquefaction susceptibility mapping for a liquefaction-prone area (Inegol-Turkey)”. Environ. Geology 44(7), pp. 862–871.

TC4, ISSMFE [1999]. *“Manual for Zonation of Seismic Geotechnical hazards”*. Japanese Society of Soil Mechanics and Foundation Engineering, Tokyo.

Toprak S., T.L. Holzer, M.J. Bennett, T.E. Noce, A.C. Padovani and J.C. Tinsley [2006]. “Liquefaction hazard mapping with LPI in the Greater Oakland, California Area”. Earthquake Spectra, 22(3), pp. 693-708.

Uzielli M., S. Lacasse, F. Nadim and K.K. Phoon [2007]. “Soil variability analysis for geotechnical practice”. In T.S. Tan, K.K. Phoon, D.W. Hight & S. Leroueil (eds.), *Proceedings of the 2nd Int. Workshop on Characterisation and Engineering Properties of Natural Soils*, Vol. 3, (IS-Singapore), Taylor & Francis, London: pp. 1653-1752.

Youd, T.L., I.M. Idriss, R.D. Andrus, I. Arango, G. Castro, J. T. Christian, R. Dobry, W.D. Liam Finn, L. F. Jr. Harder, M.E. Hynes, K. Ishihara, J.P. Koester, S.S.C. Laio, Iii W.F. Marcuson, G.R. Martin, J.K.Mitchell, Y. Moriwaki, M S. Power, P.K. Robertson, R.B. Seed and Ii K.H. Stokoe [2001]. “Liquefaction resistance of soils: Summary report from the 1996 NCEER and 1998 NCEER/NSF workshops on evaluation of liquefaction resistance of soils”. Jour. Geotech. Geoenviron. Eng., 127(10), pp. 817–833.